Regular Paper

Automatic Viewpoint System to Eliminate Blind Spots in Remote Drone Operation Using Virtual Third-Person View

Reo Akamine*, Noriaki Takenoue**, and Yuichi Tokunaga*

*Graduate School of Engineering, Kanazawa Institute of Technology, Japan
**GSEC Inc., Japan
{c6301767@st, y.tokunaga@neptune}.kanazawa-it.ac.jp,
takenoue@gsec.biz

Abstract - We propose a third-person view (TPV) system that allows a remote drone operator to easily detect the surroundings of a drone in a virtual space. However, when the virtual viewpoint is fixed, obstacles and the drone itself can cause blind spots, making it difficult for the remote operator to determine the circumstances in the blind-spot area. To solve this problem, we aimed to minimize blind spots by automatically operating a virtual viewpoint and improving flight safety. We developed an automatic search method for the virtual viewpoint that minimizes the blind area to capture the drone. We called this method the Adaptive Virtual Viewpoint (AVVP) algorithm. In this method, the blind-spot time is managed in units of 3D grids, and the movement path of the virtual viewpoint is determined. We improved the proposed algorithm and evaluated three different algorithms. The best algorithm gave weight to the angle between the virtual viewpoints. This algorithm eliminated blind spots and prevented sudden changes in the direction of virtual viewpoints.

Keywords: remote operation, drone, blind spot, third-person view, digital twin

1 INTRODUCTION

In the Japanese logistics industry, the amount of work per worker is increasing because of the increase in small-lot deliveries and strict customer delivery-time requirements. Consequently, the working environment has deteriorated and created a shortage of manpower [1]. A similar phenomenon has been observed overseas [2][3]. Specifically , an American corporation known as Driver Solutions was established to offer truck driving training for individuals to obtain commercial driver licenses [4]. In Australia, a platform called Women in Transport Network was established to increase the number of female employees [5]. In Japan, measures for reducing the number of redeliveries include installing home delivery boxes and improving working conditions, pay, and welfare benefits. Additionally, much attention is also being paid to delivery services that use drones.

Drones have been proposed to provide various services [6], such as delivery, agricultural, disaster relief, and essential infrastructure monitoring services [7]. Drone delivery services are expected to play an active role in the last mile. The last mile is the section from the final logistics base to the end user. Amazon introduced the Amazon Prime Air drone delivery service [8]. Various countries are developing legislation to regulate drone use. In the United States, the Federal Aviation Administration has approved the registration of drones on a dedicated website and the operation of drones flying at altitudes of 400 ft or less [9]. Other countries have made similar progress.

In Japan, the Civil Aeronautics Law was amended in December 2022 allowing flights beyond visual lines of sight in populated areas and making drone operations possible in urban settings [10]. Companies and local governments collaborate in demonstration experiments for the drone delivery of pharmaceuticals and lightweight packages and for flights beyond visual lines of sight. However, complex building structures and utility poles in urban areas pose obstacles that complicate drone operations. In 2023, the number of reported accidents reached 447, of which 89 were classified as severe incidents [11]. The reported accidents included contact with power lines and collisions between buildings and vehicles. Numerous incidents of contact with other people have been reported, raising the possibility of similar issues in Japan.

To address this issue, we propose a virtual third-person view (TPV) system for remotely piloting drones [12]. Through virtual reality (VR) imagery, the system allows users to determine the spatial relationship between the piloted drone and the surrounding obstacles. Our research assumed the presence of a pilot; however, research on autopilot drone systems is increasing, but accepting the risks of unmanned drones is difficult [13]. Remote operators of aircraft with unmanned systems tend to be less willing to accept the risks of modern drone technology. At the same time, there are parties involved, such as drone operators, who would take responsibility in the event of a severe accident [14]. Safe aviation requires minimizing human error and taking advantage of human concepts such as flexibility, goal awareness, and common sense.

As a prerequisite for remote human operation, essential information must be visual. In this context, virtual systems can provide satisfactory information. However, in cases where the virtual viewpoint is fixed, the aircraft itself acts as a visual hindrance, creating blind spots that may affect hazard perception. Therefore, for safe remote operation, it is necessary to make these blind spots observable to remote operators. In this study, to eliminate blind spots that occur

when operating a drone, we constructed a virtual viewpoint search algorithm using 3D grid management in a virtual space and evaluated the effect of eliminating blind spots by moving the viewpoint along different courses.

2 RELATED WORK

2.1 Blind Spots Detection Method

Blind spots pose a significant threat to the safe operation of mobile devices. For example, automated vehicles are unable to detect hazards in blind spots [15], and fatal construction accidents have occurred during the operation of heavy equipment owing to blind spots [16]. If blind spots are temporary, they can be eliminated immediately; however, if they persist for a long time and are difficult to recognize, accidents may occur. This is called the collision course phenomenon and is considered dangerous in all forms of mobility, including cars, airplanes, and ships [17][18].

Figure 1 shows the blind-spot detection methods. Blind-spot detection technology is broadly classified into detection using sensors and visual recognition. For example, ultrasonic sensors are used to monitor vehicles that cannot be observed through side mirrors [19]. In their study, potential risks were defined at three levels, and LEDs corresponding to each risk were activated based on distance data obtained from ultrasonic sensors. To prevent accidents between large vehicles such as trucks and pedestrians hidden by blind spots, Bluetooth low energy and a received signal strength indicator were used to warn both drivers and pedestrians of danger [20]. In their study, attachable LED lights and vibration motors were used to warn drivers and pedestrians of each other's presence. This method for detecting blind spots relies on the use of sensors which may malfunction; therefore, the visual recognition of blind-spot areas is also important.

The two visualization methods are drones and virtual space utilization. Inoue et al. developed a remote drone operation system, BirdViewAR, as a spatial recognition assistant for remote pilots during drone operation [21]. BirdViewAR reveals the surroundings of a drone by controlling a secondary tracking drone in response to the speed and direction of the maneuvered drone. The tracking drone provides a TPV to assist the remote pilot in controlling the primary drone. The screen provided has an additional augmented reality (AR) overlay to enhance the spatial awareness of the piloted drone and its surroundings. In their study, three patterns were evaluated: first-person view (FPV), BirdView without AR, and BirdViewAR. They found that BirdViewAR performed better in both spatial recognition and maneuvering performance. However, issues remain in ensuring the safety of tracking drones that provide TPV images. In a similar study, Temma et al. used a tracking drone to provide a TPV to enhance the pilot's understanding of the drone's surroundings but described safety issues with the tracking drone [22]. The use of drones for visualization does not address safety issues; therefore, a method that utilizes virtual space is proposed.

Takeuchi et al. used pre-mapped three-dimensional spatial information to make obstacles that cause blind spots transparent for narrow-space exploration within blind-spot

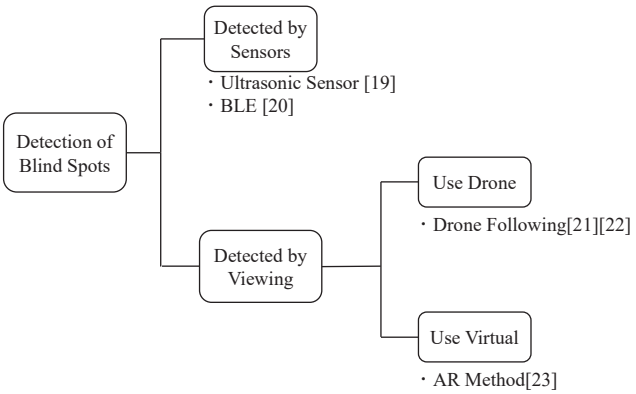

Figure 1: Blind- spot detection method

areas [23]. They proposed two methods for recognizing obstacles around a drone at a transparent destination and compared them with conventional methods. In their experiment, subjects wore headsets and pilot drones behind walls using an AR-based TPV. The AR-based method improved the drone maneuverability compared with that of conventional methods. However, if obstacles that cause blind spots are displayed transparently, the operator may have difficulty accurately perceiving the distance between the drone and the obstacle. In this case, the operator must change their position and check the spatial relationship from a different angle.

2.2 Automatic Viewpoint Movement

Moving the viewpoint to verify the relationship between the drone and obstacles from different angles can increase the operator's workload. Therefore, technologies that can automatically move viewpoints are required. For example, autonomous cameras that adapt to a surgeon's movements using machine learning [24] and methods that present a viewpoint adapted to the operator to assist in the remote operation of a robot [25] are available. These methods are suitable for presenting viewpoints in environments in which the operator's work pattern is fixed. However, they are not adaptable to the high degrees of freedom of drone flights.

Thomason et al. automatically detected dangerous obstacles and made the pilot aware of the positional relationship between a drone and obstacle by moving the viewpoint in a VR environment [26]. In their study, when the virtual drone detected an obstacle, the camera position changed according

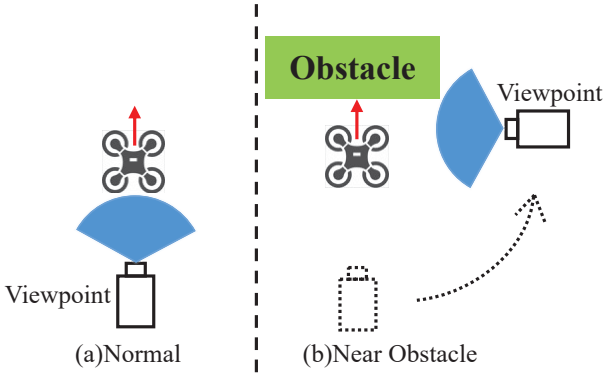

Figure 2: Automatic adjustment for virtual viewpoint

to the situation. For example, if there is no danger, the virtual viewpoint follows the drone and is positioned 3 m behind it (Fig. 2(a)). On the other hand, if the drone approaches an obstacle, the virtual viewpoint moves between the drone and the obstacle to clearly show the positional relationship between the drone and the obstacle (Fig. 2(b)).

The subjects wore headsets and flew a drone using only the VR video to compare the effectiveness of the FPV and TPV viewpoints. The results demonstrated the effectiveness of automatic viewpoint movement during maneuvering as it reduced the number of obstacle collisions compared to that of FPV or TPV. However, although this method was designed for obstacle avoidance, obstacles that are always present are likely to be handled safely based on the pilot's experience. However, there is a risk that the system may misjudge sudden obstacles. Therefore, relying on machines to judge obstacles is not an appropriate solution.

As described above, there have been many related studies on the use of virtual spaces for blind-spot detection and automatic viewpoint adjustment. However, even if temporary blind spots can be eliminated, some blind spots remain difficult to recognize. For example, the collision course phenomenon can be difficult to notice, as it creates a situation where an approaching object remains unnoticed for a long time.

3 PROPOSAL METHOD

3.1 Architecture for Automatic Viewpoint Movement

In our proposal to eliminate blind spots, we propose the Adaptive Virtual Viewpoint (AVVP) algorithm, an algorithm that detects areas where blind spots appear in the virtual space and finds the viewpoint that minimizes the duration of the blind spot. Specifically, the space is divided into 3D grids of a defined size, and the durations of the blind spots are managed on a grid-by-grid basis. The sum of the durations across all grids is used as the blind-spot cost, and the virtual viewpoint with the lowest blind-spot cost is chosen as the next virtual viewpoint. However, because a large viewpoint shift can disturb the pilot's situational awareness, we aim to select a virtual viewpoint with both a low blind-spot cost and minimal shift to prevent such disturbances.

Figure 3 shows the process flow from virtual space generation to viewpoint shift. Information on blind-spot costs was managed through the grid-based management of blind spots, and blind-spot detection was performed based on this information. To find a new virtual viewpoint, the system searches for viewpoint candidates for the next position that can most effectively reduce accumulated blind-spot costs.

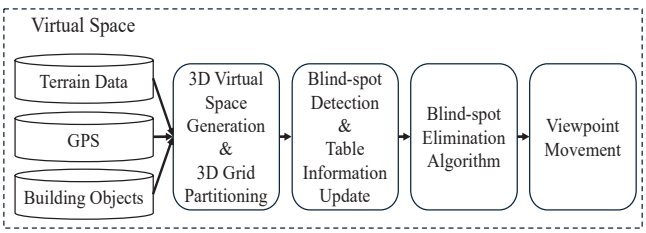

Figure 3: Architecture for AVVP algorithm

Table 1: Management table information

Management Information	Type	Description
Position	**Tuple**	**Grid Coordinate**
Building	**Bool**	**Presence of Building**
Drone	**Bool**	**Presence of Drone**
BlindParameter	**Float**	**Elapsed Time of Blind Spot**

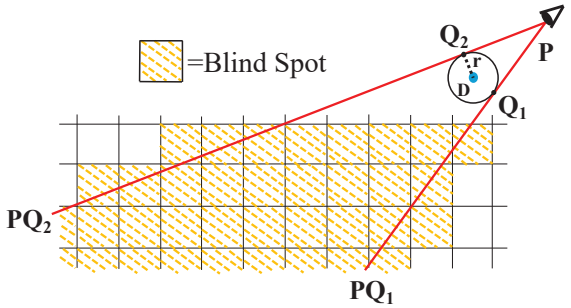

Figure 4: Image of blind-spot detection

3.2 3D Grid Partitioning

3D grids were generated by dividing the progenerated 3D virtual space to manage the blind spots. Each grid generates a table that can manage a "BlindParameter" called the blind-spot cost, along with the location information of the corresponding building, the presence or absence of a virtual viewpoint or drone (Table 1). The position coordinates stored in the table are calculated relative to the absolute coordinates of the virtual space. The grid size can be freely set; however, the grid size must be set appropriately because it affects the amount of viewpoint movement, and the time required to search for blind spots.

Let i be the total set of divided grids and j be the area where the virtual viewpoint can detect blind spots. Area j, referred to as the view area, is defined as a region centered on the drone's coordinates, with a predetermined size. Additionally, a set k of grids exists that are judged as blind spots in the viewing area. The relation between the total set i, the view area j, and the blind-spot set k is expressed by (1).

$$k \in j \in i \tag{1}$$

3.3 Blind-Spot Detection

In this study, we detected blind spots caused by the drone hindering visibility in virtual space. The drone is represented as a sphere with radius r centered at the drone's position D, and blind-spot detection is performed within the view area j.

As shown in Fig. 4, the grids inside the straight lines PQ_1 and PQ_2, which are the boundary lines passing through the virtual viewpoint P and the surface coordinates of the spheres Q_1 and Q_2, were determined to be blind spots. Here, for the purpose of eliminating all hazards, grids touching the boundary lines are also classified as blind spots. When the viewpoint was closer to the drone, the blind-spot area

increased, whereas when the distance was greater, the blind-spot area decreased.

Grids identified as blind spots have an increased blind-spot cost value in the grid management table. The cost value was weighted using a weight $w(Distance)$ assigned based on the distance between the virtual viewpoint and each grid. To prioritize the elimination of blind spots in grids closer to the virtual viewpoint, a higher weight was assigned to these grids. As the distance from the virtual viewpoint increased, the priority for blind-spot elimination decreased.

Additionally, let a_k represent the total sum of grids within the view area j that were identified as blind spots. This value is defined as

$$a_k = \Sigma_{x \in j} m_k(x) \cdot w\big(Distance(P, x)\big) \tag{2}$$

where $w(Distance(P, x))$ represents the weight based on the distance from viewpoint P to grid x.

The calculated total number of blind-spot determinations, a_k, is considered the blind-spot cost and is used to derive a new virtual viewpoint position aimed at resolving the existing blind spots.

The function m_k indicates whether grid x belongs to the set of blind spots k, and it is defined as follows.

$$m_k(x) = \begin{cases} 1 & if\ x \in k \\ 0 & if\ x \notin k \end{cases} \tag{3}$$

3.4 Blind-Spot Elimination Algorithm

To reduce the detected blind-spot area, it is necessary to move the current virtual viewpoint to a new position. Set L is defined as the set of adjacent grids that include the current virtual viewpoint, and the new virtual viewpoint is selected from this set.

From set L, we search for a new virtual viewpoint that can eliminate the largest number of blind spots. As a search method, we performed a blind-spot judgment within the new viewing area j' from the viewpoint candidate P_l. Here, the set of blind spots determined in the viewing area is kP_l.

Next, the complement set $\overline{kP_l}$ is obtained by excluding the blind-spot set kP_l from set i of the grids as

$$\overline{kP_l} = i - kP_l, l \in L \tag{4}$$

Equation (4) shows the part excluded from the viewing area j', that is, the set that is not a blind spot. Next, the common set between the blind-spot set k at the previous virtual viewpoint P and the complement set $\overline{kP_l}$ is determined. This is called S_{P_l} and is defined as

$$S_{P_l} = k \cap \overline{kP_l} \tag{5}$$

Equation (5) represents the set that was determined to be a blind spot at the previous virtual viewpoint P but was not determined to be a blind spot from the new virtual viewpoint. The total cost of this set is called the blind-spot elimination cost, $C(P_l)$, which is the cost of the blind spot that occurred at the previous virtual viewpoint P.

The new virtual viewpoint P_{adp} is the one that achieves the maximum blind-spot elimination cost, $maxC(P_l)$. In addition, $maxC(P_l)$ is evaluated using a cost function.

$$C(P_l) = \Sigma S_{P_l} \tag{6}$$

$$maxC(P_l) > 10 \cdot n \tag{7}$$

$$P_{adp} = argmaxC(P_l) \tag{8}$$

The variable n in Equation (7) represents the number of steps taken to explore the new virtual viewpoint P_{adp}. A higher number of steps indicates that the new virtual viewpoint P_{app} moved farther from the previous virtual viewpoint P. This cost function was designed to prevent excessive movement.

Finally, if the grids determined to be blind spots at the previous virtual viewpoint P remained at the new virtual viewpoint P_{adp}, they were used as parameters to determine the new virtual viewpoint P_{app}. This process yields the total blind-spot cost a'_k. Additionally, if the time step t is greater than or equal to 1, the cumulative blind-spot cost $X(i,t)$ is incremented by this value. Equation (9) is used to calculate the total blind-spot cost, and Equation (10) is used to calculate the cumulative blind-spot cost.

$$a'_k = a_k - argmaxC(P_l) \tag{9}$$

$$X_{i,t+1} = X_{i,t} + a'_k, t \geq 1 \tag{10}$$

The new virtual viewpoint P_{app} obtained by Equation (8) is moved from the previous virtual viewpoint P to provide the pilot with a new virtual viewpoint.

3.5 Viewpoint Movement

The Slerp method was used to ensure a smooth transition of motion between a new virtual viewpoint and the previous virtual viewpoint. Slerp utilizes a technique called quaternion, which efficiently handles rotations in a 3D space to perform interpolation on the surface of a sphere [27]. This allows for the creation of a natural and smooth trajectory between the previous and new virtual viewpoints.

Slerp were used to find new virtual viewpoints and eliminate blind spots.

4 EVALUATION

4.1 Evaluation Method

To verify the effectiveness of the proposed AVVP algorithm, we used the prepared scenario to explore new virtual viewpoints. The viewpoint paths and the blind-spot elimination rates obtained from three different algorithms were then evaluated:

(A) proposed virtual viewpoint search AVVP algorithm,
(B) algorithm with an added function to predict the movement of the drone, and
(C) algorithm with an added function to predict drone movement and new weighting function.

Table 2: Parameters used for evaluation

Variable	Parameter
Virtual Space Area	50(m)
3D Grid Size	1(m)
View Area Size	20(m)
Radius of a Sphere	0.5(m)

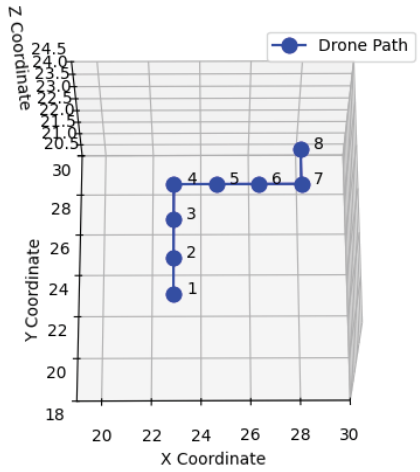

Figure 5: Path of drone

Parameters such as the size of the view area and 3D grid are required to search for new virtual viewpoints, and these details are listed in Table 2. In addition, the weight value based on the distance between the virtual viewpoint and each 3D grid detected as a blind spot in the algorithm is given by Equation (11). The values of these parameters were set intuitively.

$$w(Distance) = \begin{cases} 1.0 & if\ 0.00 \leq Distance \leq 5.00 \\ 0.8 & if\ 5.01 \leq Distance \leq 6.00 \\ 0.6 & if\ 6.01 \leq Distance \leq 7.00 \\ 0.4 & if\ 7.01 \leq Distance \leq 8.00 \\ 0.2 & if\ 8.01 \leq Distance \leq 9.00 \\ 0.1 & if\ Distance > 9.00 \end{cases} \quad (11)$$

The three algorithms used for evaluation were evaluated under the following scenario of a drone path experiencing a sudden change in the direction as shown in Fig. 5:

・the same initial position of virtual viewpoint was set for each algorithm, and

・the virtual viewpoint field of view was set at 120°.

First, we evaluated using Algorithm (A) as proposed in the previous section.

4.2 Evaluation of the No-Movement-Prediction-Algorithm

Figures 6 and 7 show the results of searching for a new virtual viewpoint using Algorithm (A). Figure 8 shows a graph of the elimination rate of blind spots for each virtual viewpoint. Figure 6 shows the movement of the drone and virtual viewpoint on the XY-plane, and Fig. 7 shows the movement of the virtual viewpoint in the Z-axis direction relative to the XY-plane. In this case, the initial position of the virtual viewpoint was set to one.

From these figures, the blind spots at each point were eliminated; however, the issue of a new virtual viewpoint path being searched for sudden changes became apparent. Although this rapid change contributes to the elimination of blind spots, it can be a significant burden on the remote operator and may impair the maneuverability of the drone.

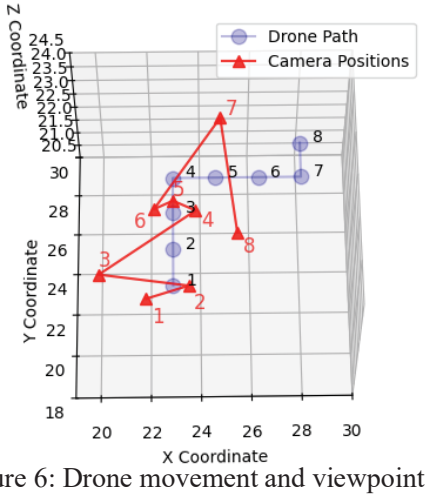

Figure 6: Drone movement and viewpoint path (top view)

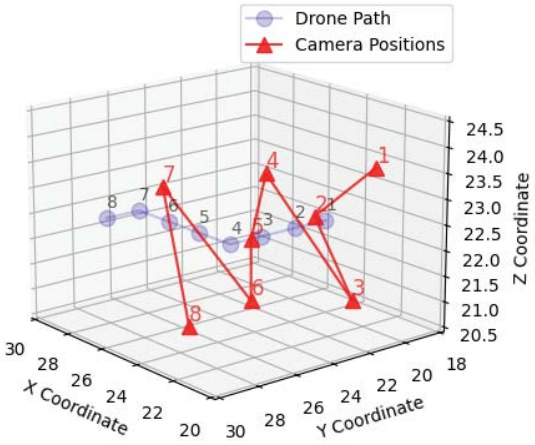

Figure 7: Drone movement and viewpoint path (side view)

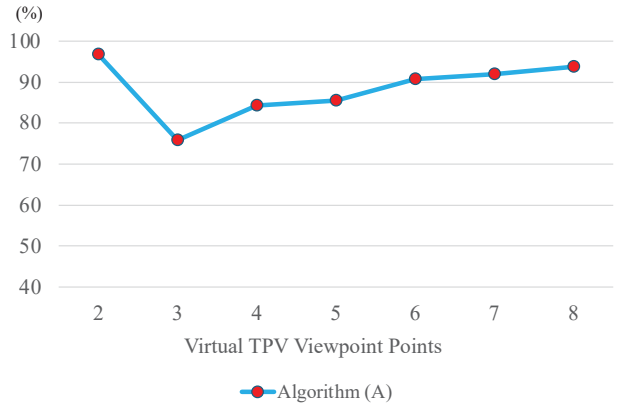

Figure 8: Algorithm (A) blind-spot elimination rate

We installed a drone-movement prediction function to suppress rapid changes in the virtual viewpoint path. This prediction function uses the most recent drone movement data to predict the distance of movement and angle of change in direction. This is expected to enable the virtual viewpoint to be searched based on the predicted drone coordinates and for the virtual viewpoint path to follow the predicted drone movement direction.

4.3 Evaluation of Algorithms with Movement Prediction

The results of the drone movement prediction function and the new virtual viewpoint search are shown in Fig. 9, 10, and 11, and a graph of the elimination rate of blind spots at each point compared to Algorithm (A) as shown in Fig. 12. In Fig. 9, the numbers with dashed marks indicate the results of the predicted drone movement. When these results match the actual movement trajectory of the drone, the prediction is accurate. Furthermore, Fig. 10 shows the movement of the drone and virtual viewpoint on the XY-plane, and Fig. 11 shows the movement of the virtual viewpoint along the Z-axis, relative to the XY-plane. In this case, the initial position of the virtual viewpoint was set to one.

While movement prediction was successful on a straight course, it was difficult to predict the movement at points where sudden changes in direction occurred. It was confirmed

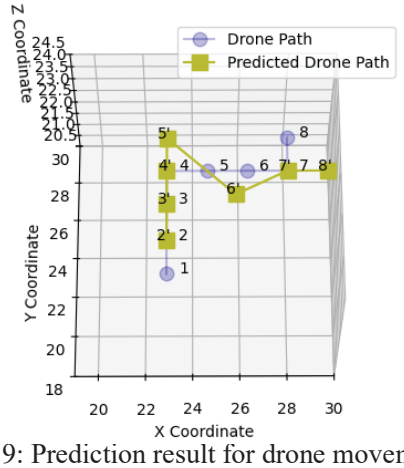

Figure 9: Prediction result for drone movement

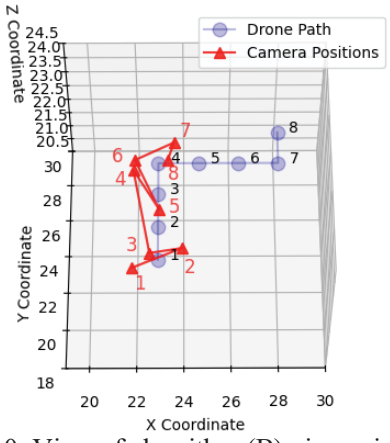

Figure 10: View of algorithm (B) viewpoint path from above

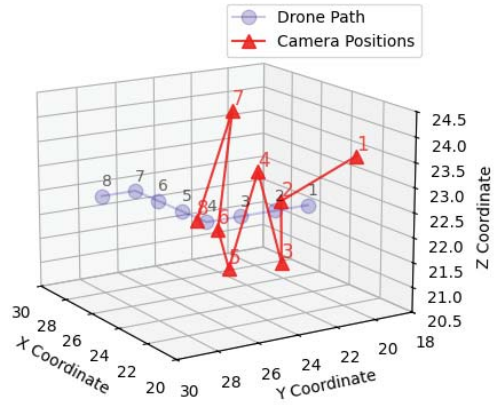

Figure 11: View of algorithm (B) viewpoint path from side

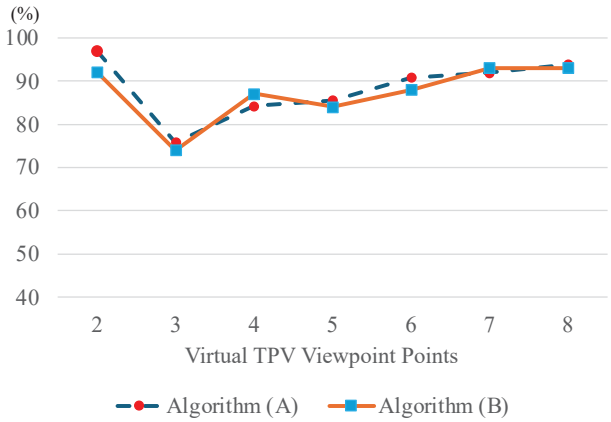

Figure 12: Algorithm (A) and (B) blind-spot elimination rates

that the virtual viewpoint was concentrated around Point 4, where the direction of travel changed suddenly, and the drone was not being followed. Figure 12 shows only a slight difference in the elimination rate of the blind spots for Algorithm (A).

The evaluation results show that the explored virtual viewpoint paths changed abruptly. To solve this problem, we set weights for the angles between virtual viewpoints when the virtual viewpoints moved. This is Algorithm (C). The weights used in Algorithm (C) are intuitively set weight values and are shown in Equation (12).

$$w(Angle) = \begin{cases} 1.0 & if\ 0 \leq Angle < 10 \\ 0.9 & if\ 10 \leq Angle < 20 \\ 0.8 & if\ 20 \leq Angle < 30 \\ 0.7 & if\ 30 \leq Angle < 40 \\ 0.6 & if\ 40 \leq Angle < 50 \\ 0.5 & if\ 50 \leq Angle < 60 \\ 0.4 & if\ 60 \leq Angle < 70 \\ 0.3 & if\ 70 \leq Angle < 80 \\ 0.2 & if\ 80 \leq Angle < 90 \\ 0.1 & if\ Angle \geq 90 \end{cases} \quad (12)$$

By assigning weights to the angles between the virtual viewpoints, it is expected that the changes in the virtual viewpoints will be more suppressed and that sudden

fluctuations between the virtual viewpoints will be suppressed.

4.4 Evaluation of Weighted Algorithm

Figures 13 and 14 show the results of the virtual viewpoint search weighted by the angles between the virtual viewpoints. Figure 15 shows the percentage of blind spots eliminated at each point compared with Algorithms (A) and (B). Figure 13 shows the movement of the drone and the virtual viewpoint on the XY-plane, and Fig. 14 shows the movement of the virtual viewpoint in the Z-axis direction relative to the XY-plane. In this case, the initial position of the virtual viewpoint was set to one.

Consequently, we confirmed that the position of the virtual viewpoint prevented sudden changes in the virtual viewpoint path that had occurred up to this point. However, as shown in Fig. 15, a significant difference in the blind-spot elimination rate between Algorithms (A) and (B) existed, and in some cases previously eliminated blind spots were not eliminated. The blind-spot elimination rate decreased significantly at Point 8.

These results suggest a tradeoff between preventing sudden changes in the direction of the virtual viewpoint path and maximizing the blind-spot elimination rate. Specifically, although the path stability can be improved by restricting the angle between virtual viewpoints, there is a possibility that the selection of virtual viewpoints to achieve a high dead-angle elimination rate will be restricted. To resolve this tradeoff, it is necessary to have an algorithm that can appropriately adjust the balance between restricting the angle between virtual viewpoints and the dead-angle elimination rate and one that can adjust the weight values.

Furthermore, from the current virtual viewpoint, the line-of-sight of each virtual viewpoint was set such that it always captured the virtual drone directly (Fig. 16 and 17).

However, with this method, the angle of the virtual viewpoint line-of-sight changes when the virtual viewpoint moves, and the remote operator may be confused by the sudden change in the scenery. To solve this problem, we introduce a line-of-sight control algorithm that improves the line-of-sight stability.

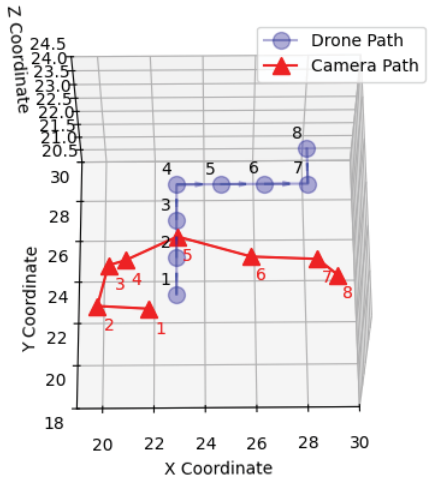

Figure 13: View of algorithm (C) viewpoint path from above

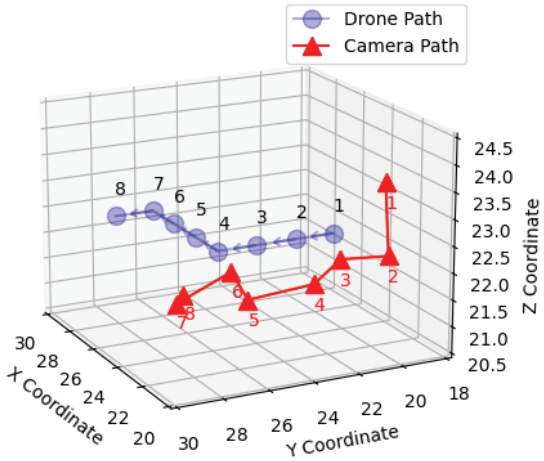

Figure 14: View of Algorithm (C) viewpoint path from the side

4.5 Evaluation of Line-of-Sight Control

In the line-of-sight control algorithm, the angle difference between the line-of-sight vector of the previous virtual viewpoint and that of the new virtual viewpoint was limited as it did not exceed half the viewing angle. It was further adjusted lower than the set angular movement amount. Through this control, we ensured that the drone images of the

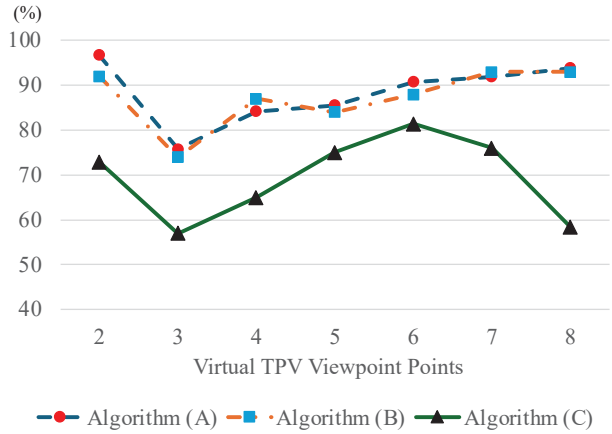

Figure 15: Comparison of algorithm blind-spot elimination rates

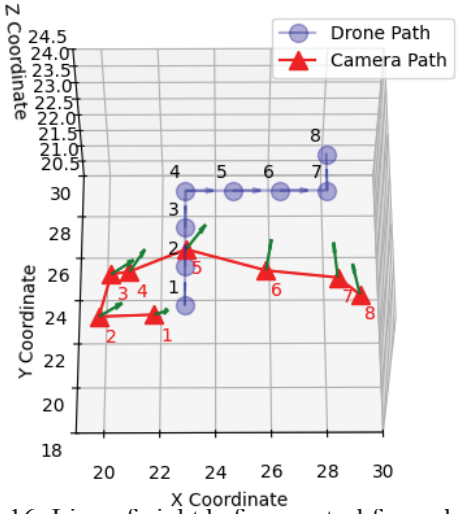

Figure 16: Line-of-sight before control from above

surroundings did not change abruptly. The viewing angle was set to 120°, and the angular movement amount was set to 10°.

Figures 18 and 19 show the line-of-sight vectors for each virtual viewpoint explored. For example, no significant change in the direction of the line-of-sight vector occurred during the line-of-sight shift from Point 6 to Point 7. In the conventional method, virtual viewpoints are continuously adjusted to look directly at the drone; therefore, the viewpoint

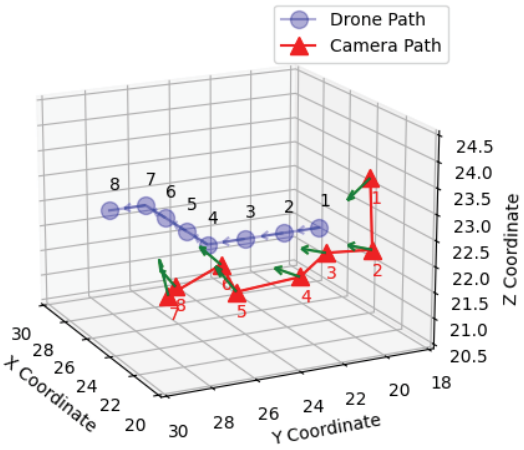

Figure 17: Line-of-sight before control from side

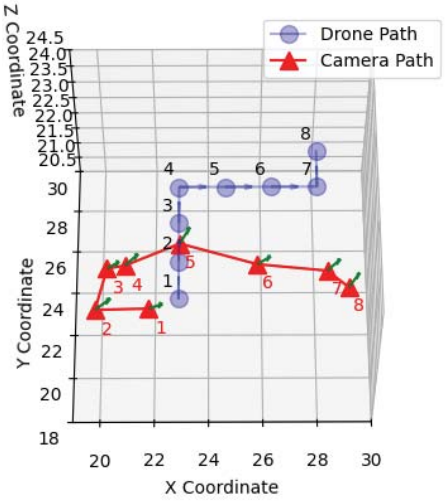

Figure 18: Line-of-sight after control from above

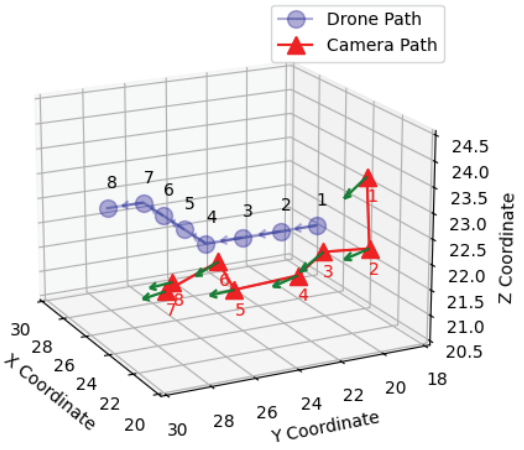

Figure 19: Line-of-sight after control from side

shift is significant. In contrast, in the proposed line-of-sight control algorithm, the maximum change between the line-of-sight vectors was 60°, and the minimum movement was within the set angular movement of 10°, which suppressed the line-of-sight shift by capturing the virtual drone within the viewing angle.

Summarizing the evaluation results, it was confirmed that the proposed algorithm searched for virtual viewpoints while prioritizing the elimination of blind spots. However, this method suffered from sudden changes in the virtual viewpoint path. In response, it was shown that assigning a weight to the angle between virtual viewpoints was effective in suppressing sudden changes in the virtual viewpoint path. However, a tradeoff exists between the blind-spot elimination rate and the suppression of sudden changes in the virtual viewpoint path. To resolve this, it is necessary to design an algorithm that can appropriately adjust the balance between the suppression of the angle between the virtual viewpoints and the blind-spot elimination rate and to adjust the weight values.

5 DISCUSSION

Furthermore, it is possible to prevent sudden changes in gaze direction by controlling the line-of-sight vector; however, several issues have become clear during the evaluation process.

First, the point at which the drone movement prediction cannot respond to changes in direction is raised. We assumed that the drone movement prediction was inaccurate. This affects the virtual search, and it is possible that an appropriate virtual viewpoint position will not be selected. We predicted changes in the drone speed and travel direction. As shown in Fig. 20, although the prediction results up to Point 8 were obtained, an error occurred during the prediction process, and the process ended halfway through. It was found that the prediction of the change in speed needed to be more accurate. For example, it was confirmed that the order of Points 7 and 8 was switched. To address these issues, we are considering a method that uses machine learning to learn past drone movement patterns and predict changes in speed and direction more accurately.

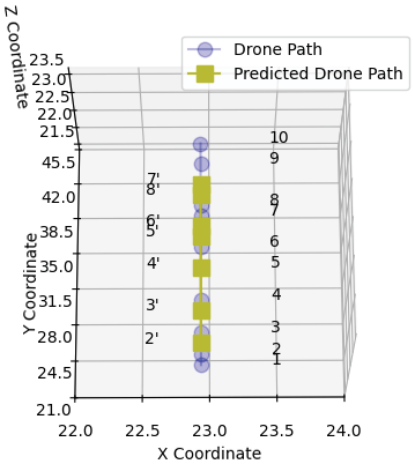

Figure 20: Prediction results for speed-change case

Next, our proposed algorithm required the setting of many parameters, such as the range of the view area, weight based on the distance between the virtual viewpoint and the blind-spot grid, and the angle of movement of the line-of-sight vector. The values of these parameters can significantly affect the evaluation results; therefore, it is necessary to establish a basis for setting the appropriate values. Adjusting these parameters appropriately and repeating the evaluation are essential to achieve safe drone operation and eliminate blind spots.

The calculation time of the algorithm was also an issue. In this algorithm, searching for a new virtual viewpoint required approximately five hours, which is a practical operational bottleneck. Long calculation times reduce the efficiency of the viewpoint search. Speeding up the calculations by parallelizing loop processing and introducing pattern memory could be a solution. It is necessary to review the algorithm and calculation procedure and consider a more efficient approach.

Finally, we address the limitations of this study. As the main objective of this research was to eliminate blind spots, the "visibility" and "way of seeing" from the explored virtual viewpoints were not considered. In this respect, even if the virtual viewpoints eliminated blind spots, they may be visually inappropriate for the remote operator. In future, it will be necessary to devise a method for exploring virtual viewpoints to improve visual comfort.

6 CONCLUSIONS

To solve the problem of manpower shortage in the logistics industry, we proposed a method of increasing the safety of drone delivery operation in urban areas by eliminating the blind spots that occur during delivery and providing blind-spot information by moving the viewpoint. Related research has presented methods for detecting blind spots in a surrounding area and freely moving viewpoints in a virtual space. However, these studies do not address the elimination of blind spots that are difficult to recognize over long periods.

We developed an AVVP(Adaptive Virtual Viewpoint) algorithm that uses a 3D grid in a virtual space to search for new virtual viewpoints and derives viewpoint paths based on a table that manages blind-spot costs and object information. To verify the effectiveness of this algorithm, we used a scenario prepared in advance to search for new virtual viewpoints and evaluate the viewpoint paths.

The evaluation confirmed that the blind-spot elimination rate was high for both the proposed algorithm and the algorithm with the drone movement prediction function; however, sudden changes occurred in the direction of the viewpoint path. By assigning weights to the angles between the virtual viewpoints, the blind-spot elimination rate decreased slightly and there was no sudden change in the direction of the virtual viewpoint path. From these results, there is a tradeoff between the suppression of sudden changes in the virtual viewpoint path and the blind-spot elimination rate, and an appropriate adjustment of the algorithm and weights is necessary to eliminate this tradeoff.

Furthermore, this study identified issues such as the insufficient prediction of changes in the speed and direction of drone flight and the length of the calculation time. However, even if the position of the virtual viewpoint eliminated the blind spot, the remote operator was not necessarily able to visualize it.

In future research, it will be necessary to develop a viewpoint search algorithm and to evaluate it quantitatively, improve the prediction accuracy and computational efficiency, and evaluate the "visibility" and "viewing" of virtual viewpoints.

REFERENCES

[1] METI, MLIT and MAFF, Current status of logistics in Japan and status of initiatives (in Japanese), https://www.meti.go.jp/shingikai/mono_info_service/sustainable_logistics/pdf/001_02_00.pdf (referred June 9 , 2024).

[2] C. Ji-Hyland and D. Allen, "What Do Professional Drivers Think about Their Profession? An Examination of Factors Contributing to the Driver Shortage," International Journal of Logistics Research and Applications, Vol. 25, No. 3, pp.231–246 (2022).

[3] J. de Winter, T. Driessen, D. Dodou and A. Cannoo, "Exploring the Challenges Faced by Dutch Truck Drivers in The Era of Technological Advancement," Frontiers in public health, Vol. 12, DOI: https://doi.org/10.3389/fpubh.2024.1352979 (2024).

[4] Driver Solutions, Driver Solutions, https://greatcdltraining.com/ (referred June 9, 2024).

[5] Victoria Government, Women in Transport Network, https://www.vic.gov.au/women-transport-network (referred June 9, 2024).

[6] L. Kapustina, N. Izakova, E. Makovkina, and M. Khmelkov, "The global drone market: Main development trends," SHS Web of Conferences, Vol. 129, p. 11004 (2021).

[7] N. Elmeseiry, N. Alshaer, and T. Ismail, "A Detailed Survey and Future Directions of Unmanned Aerial Vehicles (UAVs) with Potential Applications," Aerospace, Vol. 8, No. 12, p. 363 (2021).

[8] H. Chen, Z. Hu, and S. Solak, "Improved delivery policies for future drone-based delivery systems," European Journal of Operational Research, Vol. 294, No. 3, pp. 1181–1201 (2021).

[9] Federal Aviation Administration, FAADroneZone Access – Home, https://faadronezone-access.faa.gov/#/ (referred June 9, 2024).

[10] MLIT, Unmanned Aerial Vehicle Level 4 Flight Portal Site, https://www.mlit.go.jp/koku/level4/ (referred June 9, 2024) (in Japanese).

[11] Unmanned Aircraft Safety Division, JCAB, MLIT, Accidents and Serious Incidents, https://www.mlit.go.jp/common/001623401.pdf (referred July 18, 2024) (in Japanese).

[12] R. Akamine, N. Takenoue, and Y. Tokunaga, "Proposal of Third-Person View for Safe Drone Remote Control Operation," Proceedings of the 85th National Convention of IPSJ, Vol. 2023, No. 1, pp. 231–232

(2023) (in Japanese).
[13] J. Keebler, E. H. Lazzara, K. Wilson, and E. L. Blickensderfer, Human Factors in Aviation and Aerospace, Elsevier, (2022).
[14] P. Slovic, The perception of risk, Routledge, (2000).
[15] J. Lu et. al, , "A quantitative blind area risks assessment method for safe driving assistance," Journal of Systems Architecture, Vol. 150, DOI: 10.1016/j.sysarc.2024.103121 (2024).
[16] J. W. Hinze and J. Teizer, "Visibility-related fatalities related to construction equipment," Safety science, Vol. 49, No. 5, pp. 709–718 (2011).
[17] P. Kevin, "Constant Bearing, Decreasing Range," US Naval Institute Proceedings, Vol. 122, No. 12 (1996).
[18] JAF Mate Online, Accidents that occur despite good prospects! The dangers of the Collision Course Phenomenon, https://jafmate.jp/car/traffic_topics_20230117.html (referred June 10, 2024) (in Japanese).
[19] Z. Adnan et al., "Vehicle Blind-spot Monitoring Phenomenon using Ultrasonic Sensor," International Journal of Emerging Trends in Engineering Research, Vol. 8, No. 8, (2020).
[20] N. De Raeve et al., "A Bluetooth low-energy-based detection and warning system for vulnerable road users in the blind spot of vehicles," Sensors, Vol. 20, No. 9, p . 2727 (2020).
[21] M. Inoue, K. Takashima, K. Fujita, and Y. Kitamura, "BirdViewAR: Surroundings-aware Remote Drone Piloting Using an Augmented Third-person Perspective," Proceedings of the 2023 CHI Conference on Human Factors in Computing System, Vol. 84, No. 31, pp. 1–19 (2023).
[22] R. Temma, K. Takashima, K. Fujita, K. Sueda, and Y. Kitamura, "Enhancing Drone Interface Using Spatially Coupled Two Perspectives," IPSJ Journal, Vol. 61, No. 8, pp. 1319–1332 (2020) (in Japanese).
[23] K. Takeuchi, R. Teng, and K. Sato, "Implementation and Evaluation of a Drone-based AR Visualization Method for Narrow Space Surveillance," IPSJ Journal, Vol. 64, No. 2, pp. 614–625 (2023) (in Japanese).
[24] M. Wagner et al., "A learning robot for cognitive camera control in minimally invasive surgery, Surgical Endoscopy," Vol. 35, No. 9, pp.5365-5374 (2021).
[25] D. Rakita, B. Mutlu, and M. Gleicher, "An Autonomous Dynamic Camera Method for Effective Remote Teleoperation," Proceedings of the 2018 ACM/IEEE International Conference on Human-Robot Interaction, pp. 325–333 (2018).
[26] J. Thomason et al., "A comparison of adaptive view techniques for exploratory 3D drone teleoperation," ACM Transactions on Interactive Intelligent Systems (TiiS), Vol. 9, No. 2–3, pp. 1–19 (2019).
[27] K. Shoemake, "Animating rotation with quaternion curves," Proceedings of the 12th annual conference on computer graphics and interactive techniques, Vol. 19, No. 3, pp. 245–254 (1985).

(Received: November 17, 2024)
(Accepted: March 1, 2025)

Reo Akamine guraduated from the Faculty of Information Frontier,Kanazawa Institute of Technology. He then entered the Graduate School of Engineering at Kanazawa Institute of Technology. He is a member of the Information Processing Society of Japan.

Noriaki Takenoue guraduated from the Department of Electronic Engineering, National Defense Academy of Japan, in March 1981 and became a research assistant at the National Defence Academy of Japan in April of the same year. He was awarded a doctorate in engineering from the Graduate School of Meiji University in Octover 1986, became a professor at the National Defense Academy in August 2009, a chief researcher at Fujitsu Systems Integration Laboratories in August 2011, and an executive officer at GSEC in August 2018. He is a member of the Infomation Processing Society of Japan and IEEE.

Yuichi Tokunaga received a Ph.D. degree in science and engineering from Ritsumeikan University in 2009. He joined Mitsubishi Electric Corporation in 1990 and engaged in the R&D of the high-reliability computers, wireless sensor networks, the algorithms of time-synchronization and positioning, the network protocol for industrial applications, and data analytics for condition-based maintenance. He has been a professor at Kanazawa Institute of Technology since 2019. He is a member of the ITS steering committee of IPSJ and a member of IEEE and ISCIE.